THE NON-LOCAL AFM WATER-WAVE METHOD FOR CYLINDRICAL GEOMETRY*

M. G. BLYTH† AND E. I. PĂRĂU‡

Abstract. We develop an AFM (Ablowitz-Fokas-Musslimani) method applicable to studying water waves in a cylindrical geometry. As with the established AFM method for two-dimensional and three-dimensional water waves, the formulation involves only surface variables and is amenable to numerical computation. The method is developed for a general cylindrical surface, and we demonstrate its use for numerically computing fully nonlinear axisymmetric periodic and solitary waves on a ferrofluid column.

Key words. Ablowitz-Fokas-Musslimani method, nonlinear waves, ferrofluid column

AMS subject classifications. 76B25, 76B10

1. Introduction.

In the classical water wave problem a solution is sought describing an inviscid fluid motion with a free surface. If the fluid motion is irrotational the mathematical problem requires the solution of Laplace's equation subject to a suitable condition on the bottom in the case of finite depth, or at minus infinity in the case of infinite depth, and subject to Bernoulli's equation and the kinematic condition at the free surface. Of particular interest is the determination of the free surface itself, and the description of waves propagating along the free surface, their shape, speed, and so on.

Numerous analytical approaches have been developed for tackling this problem (for a review see, for example, Lannes [14]). In 2006 Ablowitz *et al.* [1] presented a new non-local formulation which they developed by exploiting a carefully chosen identity for harmonic functions. We shall refer to this as the AFM (Ablowitz-Fokas-Musslimani) method. This was used to re-express the problem in terms of an integral over the free surface to be solved along with Bernoulli's equation. Accordingly their formulation involves only surface variables and can therefore be solved independently and without reference to the remainder of the flow domain. This new approach has been used, for example, to study the stability of two-dimensional periodic waves on water of finite depth in the presence of gravity (Deconinck & Oliveras [8]) and in the presence of both gravity and surface tension (Deconinck & Trichtchenko [9]), and for bathymetry detection from surface data (Vasan & Deconinck [20]). It has also been extended to include vorticity (Ashton & Fokas [4]) and to two-layer flows (Haut & Ablowitz [13]). In effect the AFM formulation is a surface-variables description of the water waves problem with an implicit Dirichlet-to-Neumann operator. The performance of the AFM method against other Dirichlet-to-Neumann formulations, including the Craig-Sulem operator expansion approach, has been assessed by Wilkening & Vasan [21].

To date the AFM method has been applied to study two-dimensional and three-dimensional surface waves. In this paper we show how it can be adapted to a cylindrical geometry, and we derive the cylindrical analogue of the nonlocal surface integral of Ablowitz *et al.* [1]. By way of demonstration, we illustrate the utility of this

*Submitted to the editors 23rd August 2018.

†School of Mathematics, University of East Anglia, Norwich, NR4 7TJ, United Kingdom (m.blyth@uea.ac.uk.

‡School of Mathematics, University of East Anglia, Norwich, NR4 7TJ, United Kingdom (e.i.parau@uea.ac.uk

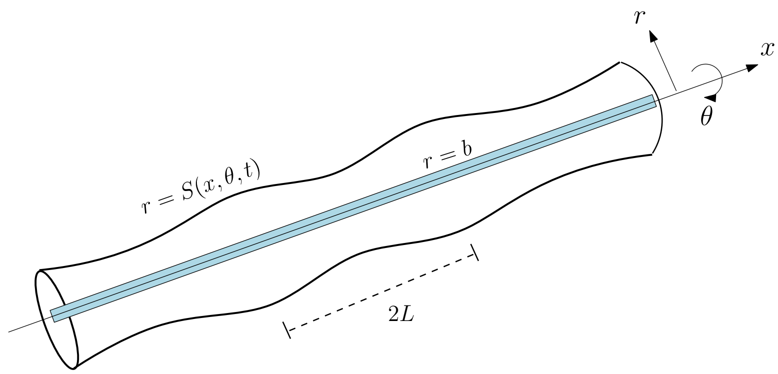

FIG. 1. *Sketch of the periodic flow geometry. The domain* Ω *occupies one wavelength* $-L \leq x \leq L$ *with* $b \leq r \leq S(x, \theta, t)$.

formulation for numerically computing fully nonlinear, axisymmetric periodic waves and solitary waves on a liquid column. Periodic axisymmetric waves on a cylindrical liquid jet have previously been computed by Vanden-Broeck *et al.* [19] using a finite difference method. While a cylindrical column will normally tend to disintegrate into droplets by virtue of the well-known Rayleigh-Plateau instability, if the liquid in question is a ferrofluid, which is essentially a stable suspension of tiny magnetizeable particles (e.g. Rosensweig [16]), the Rayleigh-Plateau instability can be resisted and the column fully stabilised when it is subjected to an azimuthal magnetic field (Arkhipenko & Barkov [3]). Such a field can be generated by placing an electric current-carrying wire or metal rod along the axis of the column. Nonlinear waves on the surface of a ferrofluid column stabilised in this way have previously been studied by Bashtovoi *et al.* [5] and Rannacher & Engel [15] using a weakly-nonlinear model equation of KdV type. Experiments confirming the possibility of periodic waves and solitary waves were performed by Bourdin *et al.* [7]. Fully nonlinear solitary wave solutions were computed by Blyth & Părău [6]. We emphasise that it is not our intention here to further the study of this physical phenomenon per se, rather to demonstrate the efficacy of the cylindrical AFM formulation for computing such waves.

2. Equations of motion. We consider a generally unsteady inviscid, incompressible and irrotational axisymmetric fluid motion with velocity $\boldsymbol{u} = \nabla\phi$, where $\phi(x, r, \theta, t)$ is the velocity potential with cylindrical polar coordinates (r, θ) and time t. The velocity potential satisfies Laplace's equation

$$\nabla^2\phi = 0, \tag{2.1}$$

in the fluid domain Ω, which we take to be cylindrical, occupying the region $b \leq r \leq S(x, \theta, t)$, $-L \leq x \leq L$, $0 \leq \theta \leq 2\pi$ for some given constants $L > 0$ and $b > 0$. The boundary $r = b$ is assumed to be a solid surface, and the boundary at $r = S(x, \theta, t)$ is assumed to be a free surface whose particular form is to be determined as part of the solution to the problem. With a view to later computing travelling wave solutions we henceforth adopt periodic boundary conditions at the domain ends $x = \pm L$. Solitary wave solutions can be computed within this framework by considering L to be sufficiently large.

Bernoulli's equation holds at the free surface so that

$$\phi_t + \frac{1}{2}\left(\phi_x^2 + \phi_r^2 + \frac{1}{r^2}\phi_\theta^2\right) + \frac{\gamma\kappa}{\rho} - V = \mathcal{E}(t), \tag{2.2}$$

at $r = S$, where γ is the surface tension at the free surface, κ is the curvature of the free surface, ρ is the fluid density, V represents a potential field associated with one or more body forces per unit mass that are influencing the fluid motion, and $\mathcal{E}(t)$ is the Bernoulli constant. The kinematic condition at the free surface requires that $D(r - S)/Dt = 0$, where D/Dt is the material derivative, which yields the condition

$$S_t + \phi_x S_x + \phi_\theta \frac{S_\theta}{S^2} = \phi_r \tag{2.3}$$

on $r = S$. On the solid boundary we enforce the impermeability condition $\phi_r = 0$ at $r = b$.

Our goal is to reformulate the problem in terms of free surface variables only. Following the approach of Ablowitz *et al.* [1], we start by noting that, if two functions $\phi(x, r, \theta, t)$ and $\psi(x, r, \theta, t)$ both satisfy Laplace's equation, then it is the case that

$$\begin{aligned}\partial_r(\phi_x\psi_r + \psi_x\phi_r) + \frac{(\phi_x\psi_r + \psi_x\phi_r)}{r} + \frac{1}{r}\partial_\theta\left(\phi_x\frac{\psi_\theta}{r} + \psi_x\frac{\phi_\theta}{r}\right)& \\ + \partial_x\left(\phi_x\psi_x - \phi_r\psi_r - \frac{1}{r^2}\phi_\theta\psi_\theta\right) &= 0\end{aligned} \tag{2.4}$$

as can be readily checked by expanding the brackets. The identity (2.4) is in divergence form which motivates us to introduce the intermediary vector field

$$\boldsymbol{a} = \left(\phi_x\psi_x - \phi_r\psi_r - \frac{1}{r^2}\phi_\theta\psi_\theta\right)\boldsymbol{e}_x + (\phi_x\psi_r + \psi_x\phi_r)\,\boldsymbol{e}_r + \left(\phi_x\frac{\psi_\theta}{r} + \psi_x\frac{\phi_\theta}{r}\right)\boldsymbol{e}_\theta, \tag{2.5}$$

where $\boldsymbol{e}_x$, $\boldsymbol{e}_r$, and $\boldsymbol{e}_\theta$ are the unit vectors in the x, r, and θ directions respectively. Choosing ϕ to be the velocity potential and applying the divergence theorem to the vector field $\boldsymbol{a}$ over the domain Ω we obtain

$$\begin{aligned}\int_0^{2\pi}\int_{-L}^{L} S\Bigg[(\phi_x\psi_r + \psi_x\phi_r) - S_x\left(\phi_x\psi_x - \phi_r\psi_r - \frac{1}{S^2}\phi_\theta\psi_\theta\right)& \\ - \frac{S_\theta}{S^2}(\phi_x\psi_\theta + \psi_x\phi_\theta)\Bigg]_{r=S}\mathrm{d}x\,\mathrm{d}\theta - b\int_0^{2\pi}\int_{-L}^{L}[\phi_x\psi_r]_{r=b}\,\mathrm{d}x\,\mathrm{d}\theta &= 0,\end{aligned} \tag{2.6}$$

where we have enforced the impermeability condition at $r = b$.

Inspired by Ablowitz *et al.* [1], we now choose for ψ the particular solution of Laplace's equation

$$\psi = \mathrm{e}^{\mathrm{i}(kx+m\theta)}F(r) \tag{2.7}$$

with

$$F(r) = \big[kbK_{m+1}(kb) - mK_m(kb)\big]I_m(kr) + \big[kbI_{m+1}(kb) + mI_m(kb)\big]K_m(kr), \tag{2.8}$$

where I_m, K_m are modified Bessel functions of the first and second kind (e.g. Abramowitz & Stegun [2]), m is a non-negative integer, and $k = n\pi/L$ for integer $n = \pm 1, \pm 2, \cdots$.

We note that the particular form (2.7) has been devised so that the second integral in (2.6) vanishes identically.

Keeping in mind our objective of determining a set of equations of motion in terms of free surface variables only, we introduce the surface potential function $q(x,\theta,t) \equiv \phi(x,S,\theta,t)$. By straightforward differentiation

$$q_x = \phi_x + S_x\phi_r, \qquad q_\theta = \phi_\theta + S_\theta\phi_r, \qquad q_t = \phi_t + S_t\phi_r, \tag{2.9}$$

where the terms on the right hand sides are evaluated at the surface $r = S$. Utilising these relations together with the kinematic condition (2.3), and assuming (2.7), the integral expression (2.6) becomes

$$\int_0^{2\pi}\!\!\int_{-L}^{L} S\Big[\mathrm{i}F(S)\Big(kS_t + \frac{m}{S^2}(q_xS_\theta - q_\theta S_x)\Big) + q_xF'(S)\Big]\,\mathrm{e}^{\mathrm{i}(kx+m\theta)}\,\mathrm{d}x\,\mathrm{d}\theta = 0. \tag{2.10}$$

Equation (2.10) represents the central equation of motion and it is expressed purely in terms of surface variables. It is the cylindrical analogue of equation (I) in Ablowitz *et al.* [1].

At this point in the interest of simplicity we specialise to axisymmetry and assume from here on that all variables are independent of θ. The particular solution (2.7) reduces to

$$\psi = kb\Big(K_1(kb)I_0(kr) + I_1(kb)K_0(kr)\Big)\mathrm{e}^{\mathrm{i}kx}, \tag{2.11}$$

and the central equation (2.10) simplifies to its axisymmetric form

$$\begin{aligned}\int_{-L}^{L} kS\Big[\mathrm{i}S_t\Big(K_1(kb)I_0(kS) + I_1(kb)K_0(kS)\Big)\\ + q_x\Big(K_1(kb)I_1(kS) - I_1(kb)K_1(kS)\Big)\Big]\mathrm{e}^{\mathrm{i}kx}\,\mathrm{d}x = 0.\end{aligned} \tag{2.12}$$

Following Wilkening & Vasan [21] we may write this as

$$\begin{aligned}\int_{-L}^{L} \mathrm{e}^{\mathrm{i}kx}S\Big(K_1(kb)I_0(kS) + I_1(kb)K_0(kS)\Big)\mathscr{N}(x)\,\mathrm{d}x\\ = \int_{-L}^{L} \mathrm{i}\mathrm{e}^{\mathrm{i}kx}\,S\Big(K_1(kb)I_1(kS) - I_1(kb)K_1(kS)\Big)\partial_x\mathscr{D}(x)\,\mathrm{d}x,\end{aligned} \tag{2.13}$$

where $\mathscr{D}(x) \equiv q(x)$ is the Dirichlet surface data, and $\mathscr{N}(x) \equiv S_t$ is the Neumann surface data. As was pointed out by Wilkening & Vasan [21] this implicitly assumes that it is possible to connect the Dirichlet and Neumann data via an infinite series expansion in terms of the basis functions (2.11); for the two-dimensional case see equations (2.5), (2.6) of [21].

Written in terms of the surface variables, the axisymmetric form of Bernoulli's equation (2.2) is given by

$$q_t + \frac{1}{2}q_x^2 - \frac{1}{2}\frac{(S_t + S_xq_x)^2}{1+S_x^2} + \frac{\gamma\kappa}{\rho} - V = \mathcal{E}(t). \tag{2.14}$$

Equations (2.12) and (2.14) constitute the equations of motion for the problem expressed in terms of surface variables only.

2.1. Travelling-wave solutions. To compute travelling-wave solutions we introduce the change of variables $(x,t) \mapsto (z,t)$, where $z = x - ct$ for constant wave speed $c > 0$. In the new variables, the Bernoulli condition (2.14) becomes

$$q_t - cq_z + \frac{1}{2}q_z^2 - \frac{1}{2}\frac{(S_t - cS_z + S_z q_z)^2}{1+S_z^2} + \frac{\gamma\kappa}{\rho} - V = \mathcal{E}. \tag{2.15}$$

Henceforth we seek only fixed-form travelling wave solutions in which case $S_t = q_t = 0$. Introducing the travelling-wave change of variables into (2.12) we observe, as did Deconinck & Oliveras [8] for two-dimensional flow, that the resulting form can be simplified further using integration by parts. First noting the relations (e.g. Abramowitz & Stegun [2], p. 376)

$$\frac{1}{\xi}\frac{\mathrm{d}}{\mathrm{d}\xi}\Big(\xi I_1(\xi)\Big) = I_0(\xi), \qquad \frac{1}{\xi}\frac{\mathrm{d}}{\mathrm{d}\xi}\Big(\xi K_1(\xi)\Big) = -K_0(\xi), \tag{2.16}$$

we integrate the first integral in (2.12) by parts to obtain

$$\int_{-L}^{L} kS(q_z - c)\Big(K_1(kb)I_1(kS) - I_1(kb)K_1(kS)\Big)\mathrm{e}^{\mathrm{i}kz}\,\mathrm{d}z = 0. \tag{2.17}$$

Following Deconinck & Oliveras [8], we view the Bernoulli condition (2.15) as a quadratic equation for q_z, solve accordingly, and insert the solution into (2.17) to obtain the final travelling-wave form

$$\int_{-L}^{L} kS\Big[(1+S_z^2)(c^2 - 2\mathcal{F})\Big]^{1/2}\Big(K_1(kb)I_1(kS) - I_1(kb)K_1(kS)\Big)\mathrm{e}^{\mathrm{i}kz}\,\mathrm{d}z = 0, \tag{2.18}$$

where

$$\mathcal{F} \equiv \frac{\gamma\kappa}{\rho} - V - \mathcal{E}, \qquad \kappa = -\frac{S_{zz}}{(1+S_z^2)^{3/2}} + \frac{1}{S(1+S_z^2)^{1/2}}. \tag{2.19}$$

We recall that $k = n\pi/L$ with $n = \pm 1, \pm 2, \cdots$. Note that (2.18) is trivially satisfied when $k = 0$.

3. Travelling-waves on a ferrofluid column. Having established the basic equations of motion for cylindrical geometry, we next demonstrate how the formulation can be applied to a particular case study. The flow domain Ω is as described in section 2, and is assumed to be filled with a ferrofluid which experiences a body force when subjected to a magnetic field (e.g. Rosensweig [16]). The region $0 \le r \le b$ is occupied by a metallic rod carrying an electric current I in the positive x direction. Such a configuration has been realised in experiments (e.g. Bourdin *et al.* [7]). The current generates an azimuthal magnetic field $\boldsymbol{H} = I\boldsymbol{e}_\theta/(2\pi r)$. The magnetic body force in the fluid is (e.g. Rosensweig [16])

$$\chi\mu_0 \boldsymbol{H}\cdot\nabla\boldsymbol{H} = -\frac{\mu_0\chi I^2}{4\pi^2 r^3}\mathbf{e}_r, \tag{3.1}$$

where χ is the magnetic susceptibility of the ferrofluid and $\mu_0 = 4\pi \times 10^{-7}\mathrm{Hm}^{-1}$ is the magnetic permeability in a vacuum. The corresponding potential field associated with this force is

$$V = \frac{\mu_0\chi I^2}{8\pi^2 r^2}. \tag{3.2}$$

The magnetic field stabilises the ferrofluid column against the well-known Rayleigh-Plateau instability (e.g. Drazin & Reid [11]) so that, in the absence of surface disturbances, it adopts an equilibrium configuration with $S = a$, for constant a. Henceforth we nondimensionalise variables using a as the reference length scale and $(a^3\rho/\gamma)^{1/2}$ as the reference time scale. Non-dimensionalising in this way reveals the importance of two dimensionless parameters, namely the dimensionless rod radius and the magnetic Bond number,

$$b^* = \frac{b}{a}, \qquad B = \frac{\mu_0 \chi I^2}{4\pi^2 \gamma a}. \tag{3.3}$$

Henceforth we drop the asterisk on b^* for convenience.

In dimensionless form, the central equations (2.18), (2.19) become

$$\int_{-L}^{L} kS\left[(1+S_z^2)\left(\frac{c^2}{2} - \frac{1}{S(1+S_z^2)^{1/2}} + \frac{S_{zz}}{(1+S_z^2)^{3/2}} + \frac{B}{2S^2} + \mathcal{E}\right)\right]^{1/2} \times \Big(K_1(kb)I_1(kS) - I_1(kb)K_1(kS)\Big)\mathrm{e}^{\mathrm{i}kz}\,\mathrm{d}z = 0, \tag{3.4}$$

where c and S are now dimensionless

Blyth & Părău [6] computed fully nonlinear solitary wave solutions for this ferrofluid system. Doak & Vanden-Broeck [10] computed periodic waves and generalised solitary waves. In relating the results to be presented below with those found by Blyth & Parau (2014), we take the Bernoulli constant in (2.15) to be

$$\mathcal{E} = 1 - \frac{B}{2}. \tag{3.5}$$

In making a correspondence between the present work and that of Blyth & Părău [6], it is important to note that the transformation $\phi_z \mapsto \phi_z - c$ is required to map from the velocity potential used here to that adopted by BP (this explains the absence of the term $c^2/2$ seen on the right hand side of BP's (3.5) with the choice made in (3.5) for the Bernoulli constant).

Linearising (2.18) it is straightforward to show that small amplitude waves with wavenumber $k_1 = \pi/L$ propagate on the surface of the ferrofluid column with speed c_0 given by (see Arkhipenko & Barkov [3]; Blyth & Părău [6])

$$c_0^2 = \frac{1}{k_1}\left(\frac{I_1(k_1)K_1(k_1b) - I_1(k_1b)K_1(k_1)}{I_1(k_1b)K_0(k_1) + I_0(k_1)K_1(k_1b)}\right)(k_1^2 - 1 + B). \tag{3.6}$$

3.1. Numerical method. In practice we solve for free surface profiles $S(z)$ that satisfy (2.18) using a numerical method. The form (2.18) has been derived assuming periodicity with period L. Accordingly we seek periodic travelling-wave solutions as a Fourier expansion. With a view to numerical implementation we write

$$S(z) \approx S_N = \sum_{n=-N}^{N} a_n \mathrm{e}^{in\pi z/L} \tag{3.7}$$

for some specified level of truncation N, where the constant generally complex coefficients a_n are to be found. Note that since $S(z)$ is real, we must have that $a_n = a_{-n}^*$. For a wave that is even about $z = 0$ the coefficients a_n are real and in this case we

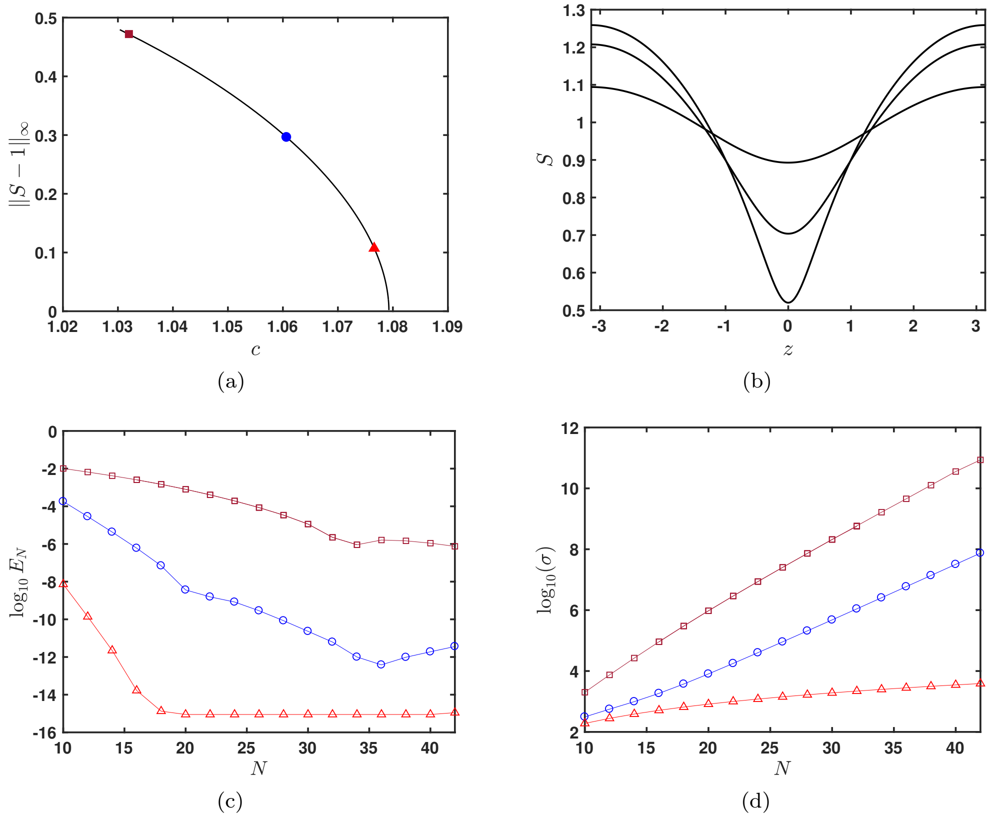

FIG. 2. *A solution branch for periodic waves of period $2L = 2\pi$ when $B = 1.5$ and $b = 0.1$: (a) the infinity norm $\|S-1\|_\infty$ against the wave speed c. The symbols correspond to $\|S-1\|_\infty = 0.107$ $(a_2 = 0.05)$ [light red $\triangle$], 0.296 $(a_2 = 0.12)$ [blue $\bigcirc$] and 0.479 $(a_2 = 0.16)$ [dark red $\square$]; (b) the wave profiles corresponding to the symbols on the branch in (a); (c) the Cauchy error $E_N = \|S_N - S_{N-2}\|_2$ at the symbols in (a); (d) the condition number $\sigma(J)$ against N for each symbol in (a).*

may replace $\exp(\mathrm{i}kz)$ with $\cos kz$ to given an entirely real expression in (2.18). All of the waves to be presented below possess this symmetry.

Substituting (3.7) into (2.18) we approximate the resulting integral using the periodic trapezium rule over a grid of equally-spaced points in the interval $[-L, L-h]$ with $h = 2L/(2N+1)$. We note that the periodic trapezium rule delivers exponential accuracy as is discussed by Trefethen & Weideman [17]. Derivatives of S are computed spectrally by taking a fast Fourier transform; products of derivatives are computed in real space. We use the zero-padding technique to mitigate against aliasing error. Setting $k = n\pi/L$ we pick n from each value in the discrete set $\{1, \ldots, N/2\}$ to obtain $2N$ algebraic equations for the $2N+2$ unknowns comprising the $2N+1$ Fourier coefficients a_n and c. A further condition comes from fixing the mean radius of the ferrofluid column so that $a_0 = 1$. One more equation is needed, and in practice we enforced a non-zero value of the second Fourier coefficient a_2 to ensure a wave of non-zero amplitude. This yields a set of $2N+2$ algebraic equations for the $2N+2$ unknowns which is solved using Newton's method for which the Jacobian J is computed numerically. All of the computations, including the calculation of the modified Bessel functions, were done in Matlab. To attempt to maintain a well-scaled Jacobian

J we divided the integrand in (2.18) by its maximum value over one period. Further discussion on this point can be found below.

As a test of our numerical procedure we repeated the two-dimensional calculations of Deconinck & Oliveras [8] using a modified form of our own code. Tests on the accuracy of the results in axisymmetry will be discussed in the next section. We also successfully recomputed some of the solitary wave solutions presented by Blyth & Părău [6].

3.2. Results. In keeping with our intention to demonstrate the efficacy of the AFM method for axisymmetric geometry, in the following two subsections we outline its capability for computing nonlinear periodic waves and solitary waves on a ferrofluid column. We note that nonlinear solutions for both periodic and solitary waves have been studied in detail elsewhere (see Doak & Vanden-Broeck [10] and Blyth & Părău [6]) using finite-difference methods.

3.2.1. Periodic waves. We may compute periodic waves using the numerical method described in section 3.1. In practice we latch onto a periodic solution branch by first computing a small amplitude wave using (3.6) to provide an initial guess for c (for chosen wavelength L) to be used in Newton's method.

Figure 2 shows a sample set of calculations for the branch of periodic waves of half-period $L = \pi$ for the case $B = 1.5$, $b = 0.1$. Panel (a) shows the solution branch characterised by the infinity norm $\|S - 1\|_\infty$ that bifurcates from the linear wave speed $c_* = 1.079$. Evidently the wave speed decreases along the branch so that $c < c_*$ for the nonlinear waves. Typical wave profiles along the branch are shown in panel (b). Numerical difficulties prevent continuation along the branch to smaller wave speeds than those shown in the figure. Ultimately we expect the waves to pinch together in the trough region to form trapped bubbles (see Doak & Vanden-Broeck [10]), similar to those seen in two-dimensional capillary and capillary-gravity waves. Since it is restricted to functions $S(z)$ which are single-valued in z it is not possible to capture such solutions with the present formulation. However as was pointed out by Wilkening & Vasan [21] for two-dimensional problems, the AFM method suffers from some ill-conditioning which appears to be the primary obstacle which frustrates continuation to larger amplitude. In particular the issue is connected with the possibility of identifying an infinite series representation for the Dirichlet and Neumann data in (2.13). In panel (c) we show the L_2-norm $E_N = \|S_N - S_{N-2}\|_2$ for increasing truncation level N. While Cauchy convergence is demonstrated for the smallest amplitude wave shown (i.e. for $a_2 = 0.05$) down to machine accuracy using double precision arithmetic, the same convergence cannot be achieved for the larger amplitude waves. The condition number $\sigma(J)$ of the Jacobian matrix J at the converged solution is plotted versus the truncation level N in panel (d) of figure 2, and it appears to be growing exponentially for the larger amplitude waves. Wilkening & Vasan [21] noted how to overcome this issue via a regularisation technique but we have not attempted to follow this here.

Figure 3(a) shows another example of a nonlinear periodic wave computed using the present method for the shorter domain $2L = \pi$ for $B = 30$ and $b = 0.1$. When the magnetic Bond number B exceeds a critical value $B_2(b)$ which depends on the rod radius, the dispersion curve for small amplitude periodic waves $c_0(k)$ versus k has a minimum (Blyth & Părău [6] – see their figure 1a). This raises the prospect of small amplitude periodic waves with two or more resonant wavenumbers for the same wave speed; this is the well-known phenomenon of Wilton ripples (e.g. Vanden-Broeck [18]). Solutions of this type can also be captured using the current method (we

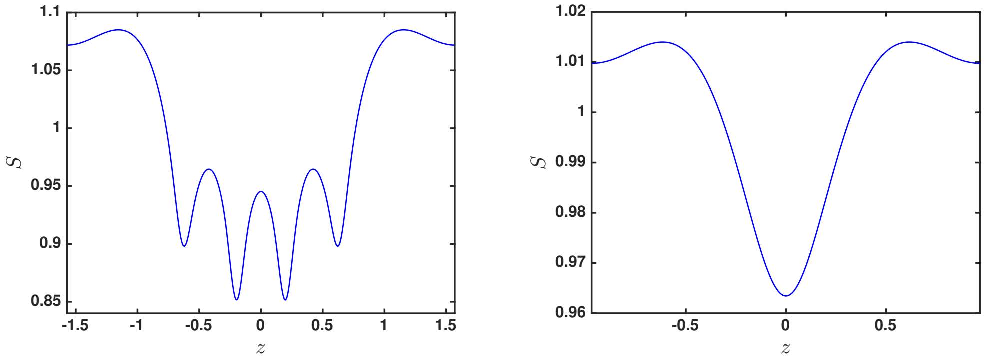

(a) (b)

FIG. 3. (*a*) *Periodic wave for* $B = 30$ *and* $b = 0.1$ *with* $2L = \pi$ *and* $c = 3.301$. (*b*) *A periodic waves with Wilton ripples for* $B = 30$ *and* $b = 0.1$ *and* $c = 3.097$ *with* $2L = 2.061 = 2\pi/k_1$ (*with* $k_1 = 3.2375$).

note that Doak & Vanden-Broeck [10] have recently computed solutions with Wilton ripples on a ferrofluid jet using a finite difference approach). In figure 3(b) we show an example of such a solution for $b = 0.1$ and $B = 30 > B_2(0.1) \approx 9$ with a 1:2 resonance meaning that linear waves with wavenumbers k_1 and $2k_1$ exist for the same wave speed c. Using the the linear theory result (3.6) we find that this occurs when $k_1 = 3.2375$ and $c = 3.173$. The solution shown in figure 3(b) lies on the solution branch which bifurcates from this point and is shown for the wave speed $c = 3.097$.

3.2.2. Solitary waves. Solitary wave solutions have previously been computed by Rannacher & Engel [15] using a weakly-nonlinear KdV model and by Blyth & Părău [6] for the fully nonlinear system. The latter authors noted that solitary waves solutions arise as bifurcations from the small amplitude periodic wave solution or as nonlinear bifurcations starting at finite amplitude. The character of the possible solitary wave solutions depends on the value of B. Indeed Blyth & Părău [6] showed that elevation solitary waves (with $S(0) > 1$) are possible in the ranges $1 < B < 2$ and $B > B_2(b)$, where the threshold value $B_2(b)$ has a closed form expression and is such that $B_2 \to 9$ as $b \to 0$. Depression solitary wave solutions (with $S(0) < 1$) are found for all $B > 1$.

We may compute solitary waves using the AFM method as follows: first we follow the branch of periodic waves emanating from small amplitude where the wave speed c satisfies (3.6); having identified a wave of some amplitude, we extend the domain L by continuation to an appropriately large value; finally, noting that our numerical procedure fixes the mean level of $S(z)$ so that in general we have attained a solitary wave with $S(\pm\infty) \neq 1$, we elevate the far-field level by continuation until $S(\pm\infty) = 1$. Figure 4(a) shows an elevation solitary wave computed in this way for $B = 1.25$ and $b = 0.1$. An example of a depression solitary wave is shown in figure 4(b). Also shown on the same graph, and barely distinguishable from the present solution, is the same wave computed using the finite difference approach of Blyth & Părău [6] (see their figure 5a).

As was noted in section 3.2.1 when $B > B_2(b)$ the linear dispersion curve has a minimum. As demonstrated by Groves & Nilsson [12] the nonlinear Schrödinger equation is a good approximation in the vicinity of this minimum and this equation

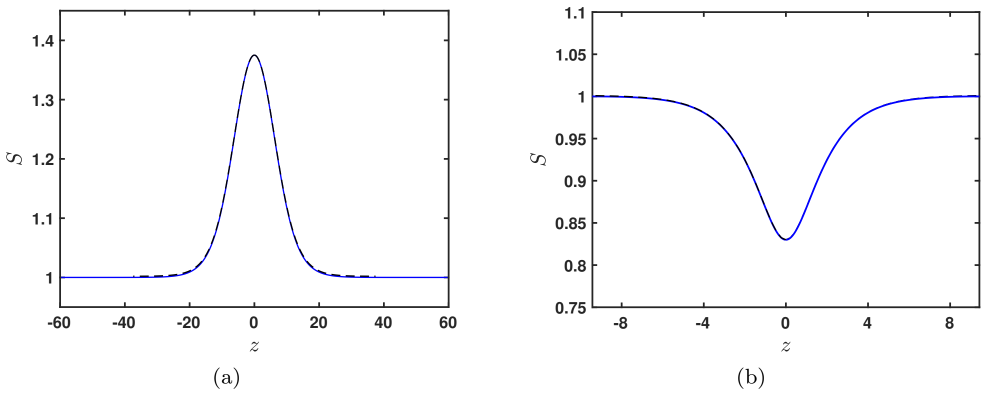

FIG. 4. *(a) Elevation solitary wave solution for $B = 1.25$ and $b = 0.1$, and (b) Depression solitary wave for $B = 4$ and $b = 0.1$. In both panels the solid line is the result computed using the present method, and the broken line is the solution of Blyth & Părău [6] shown in their figure 5a (for panel a) and their figure 6 (for panel b).*

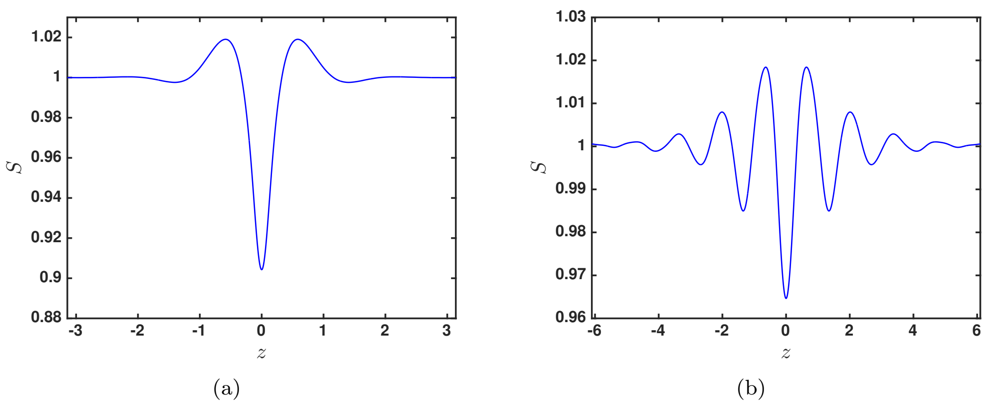

FIG. 5. *Depression solitary waves (with $S(0) < 1$) on a branch bifurcation from the minimum of the linear dispersion curve for $B = 30$ and $b = 0.1$. (a) $c = 2.918$ and (b) $c = 3.085$.*

has both elevation and depression solitary waves. Fully nonlinear solutions of both of these types were computed by Blyth & Părău [6]. Examples of depression waves of this type computed using the present AFM method are shown in figure 5. In particular the wave in panel (a) is a reproduction using the current method of that shown in figure 9(a) of Blyth & Părău [6].

4. Summary. We have developed an AFM (Ablowitz-Fokas-Musslimani) water-wave method for cylindrical geometry, and have demonstrated the use of the method for computing fully nonlinear travelling-waves on a ferrofluid column which has been stabilised by an azimuthal magnetic field. Previous studies have used finite-difference methods based on a hodograph-type approach which simplifies the domain geometry but which requires the solution of a nonlinear equation for the velocity potential. A significant drawback of such methods is that they require the discretisation of the entire fluid domain. In contrast the AFM method is formulated with reference to variables evaluated at the free surface only. While the finite-difference approach produces a discretisation error which depends algebraically on the mesh size of the computational grid, the AFM method is much simpler to implement and can achieve exponential convergence. However, as was noted above, and discussed in depth for the two-dimensional case by Wilkening and Vasan [21], the method can suffer from ill-conditioning and regularisation techniques may be needed for very high precision calculations. Nonetheless, as we have demonstrated, even for relatively large amplitude waves, a good degree of accuracy can be achieved. Moreover, the method can be readily adapted for investigating the stability of travelling-wave solutions, as was done in two-dimensions by Deconinck & Oliveras [8]. For the axisymmetric computations performed here this is left as a topic for future work.

REFERENCES

[1] M. J. Ablowitz, A. S. Fokas, and Z. H. Musslimani, *On a new non-local formulation of water waves*, J. Fluid Mech., 562 (2006), pp. 313–343.

[2] M. Abramowitz and I. A. Stegun, *Handbook of mathematical functions: with formulas, graphs, and mathematical tables*, vol. 55, Dover publications New York, 1972.

[3] V. I. Arkhipenko and Y. D. Barkov, *Experimental study of the breakdown of the cylindrical layer of a magnetizable fluid under the action of magnetic forces*, J. Appl. Mech. Tech. Phys, 21 (1980), pp. 98–105.

[4] A. C. L. Ashton and A. S. Fokas, *A non-local formulation of rotational water waves*, J. Fluid Mech., 689 (2011), pp. 129–148.

[5] V. Bashtovol, A. Rex, and R. Foiguel, *Some non-linear wave processes in magnetic fluid*, Journal of Magnetism and Magnetic Materials, 39 (1983), pp. 115–118.

[6] M. G. Blyth and E. I. Părău, *Solitary waves on a ferrofluid jet*, J. Fluid Mech., 750 (2014), pp. 401–420.

[7] E. Bourdin, J.-C. Bacri, and E. Falcon, *Observation of axisymmetric solitary waves on the surface of a ferrofluid*, Phys. Rev. Lett., 104 (2010), p. 094502.

[8] B. Deconinck and K. Oliveras, *The instability of periodic surface gravity waves*, J. Fluid Mech., 675 (2011), pp. 141–167.

[9] B. Deconinck and O. Trichtchenko, *Stability of periodic gravity waves in the presence of surface tension*, Eur. J. Mech. B/Fluids, 46 (2014), pp. 97–108.

[10] A. Doak and J.-M. Vanden-Broeck, *Travelling wave solutions on an axisymmetric ferrofluid jet*, Submitted.

[11] P. G. Drazin and W. H. Reid, *Hydrodynamic stability*, Cambridge university press, 2004.

[12] M. Groves and D. Nilsson, *Spatial dynamics methods for solitary waves on a ferrofluid jet*, J. Math. Fluid Mech., (2018), pp. 1–32.

[13] T. S. Haut and M. J. Ablowitz, *A reformulation and applications of interfacial fluids with a free surface*, J. Fluid Mech., 631 (2009), pp. 375–396.

[14] D. Lannes, *The water waves problem: mathematical analysis and asymptotics*, vol. 188, American Mathematical Soc., 2013.

[15] D. Rannacher and A. Engel, *Cylindrical korteweg–de vries solitons on a ferrofluid surface*, New J. Phys., 8 (2006), p. 108.

[16] R. E. Rosensweig, *Ferrohydrodynamics*, Courier Corporation, 2013.

[17] L. N. Trefethen and J. A. C. Weideman, *The exponentially convergent trapezoidal rule*, SIAM Review, 56 (2014), pp. 385–458.

[18] J.-M. Vanden-Broeck, *Gravity-capillary free-surface flows*, Cambridge University Press, 2010.

[19] J.-M. Vanden-Broeck, T. Miloh, and B. Spivack, *Axisymmetric capillary waves*, Wave motion, 27 (1998), pp. 245–256.

[20] V. Vasan and B. Deconinck, *The inverse water wave problem of bathymetry detection*, J. Fluid Mech., 714 (2013), pp. 562–590.

[21] J. Wilkening and V. Vasan, *Comparison of five methods of computing the dirichlet-neumann operator for the water wave problem*, Contemp. Math, 635 (2015), pp. 175–210.